

Metabolic Profiling and Outer Pericarp Water State in Zespri, Cl.GI, and Hayward Kiwifruits

Donatella Capitani,[†] Luisa Mannina,^{*,†,#} Noemi Proietti,[†] Anatoly P. Sobolev,[†] Alberta Tomassini,[‡] Alfredo Miccheli,[‡] Maria E. Di Cocco,[‡] Giorgio Capuani,[‡] Flavio Roberto De Salvador,[§] and Maurizio Delfini[‡]

[†]Istituto di Metodologie Chimiche, Laboratorio di Risonanza Magnetica “Annalaura Segre”, CNR, I-00015 Monterotondo, Rome, Italy

[#]Dipartimento di Chimica e Tecnologie del Farmaco e [‡]Dipartimento di Chimica, Sapienza Università di Roma, Piazzale Aldo Moro 5, I-00185 Rome, Italy

[§]CRA Centro di Ricerca per la Frutticoltura, Via Fioranello 5, I-00134 Rome, Italy

S Supporting Information

ABSTRACT: The metabolic profiling of aqueous extracts of Zespri Gold (*Actinidia chinensis*) and Cl.GI (a controlled crossbreed from different species of *Actinidia deliciosa*) kiwifruits and the water state of the outer pericarp of entire fruits were monitored over the season by means of high-field NMR spectroscopy and T_2 relaxation time measurements, respectively, and compared with the corresponding ones of Hayward kiwifruits previously investigated. A more complete assignment of the ^1H spectrum with respect to that obtained previously was reported: histidine, phenylalanine, quercetin 3-rhamnoside, and epicatechin were identified. Metabolic profiling confirmed Zespri's earlier maturation compared with the two other varieties. The water state of entire kiwifruits was measured nondestructively on fruits attached to the plants or detached from the plants. T_2 relaxation times were found to be sensitive to the kiwifruit developmental stage.

KEYWORDS: *Actinidia chinensis*, *Actinidia deliciosa*, kiwifruit, nuclear magnetic resonance, metabolic profiling, portable NMR, relaxation time

■ INTRODUCTION

Kiwifruit has become an important horticultural crop for its sensory and nutritional properties. As reported in the *World Kiwifruit Review* (1998, Belrose, Inc., Pulham, WA) and discussed by Ferguson,¹ “The kiwifruit industry is unique among global fruit industries in being so totally dominated by one variety, the Hayward variety.” For many years, the international success of kiwifruit has been considered to be the success of one fruiting cultivar, ‘Hayward’. Different cultivars of *Actinidia deliciosa* have been developed,¹ and different males of *Actinidia deliciosa* have been selected for the specific climatic conditions of different regions. Commercial cultivation of different *Actinidia* species with quite distinct fruits has begun to take hold. In this context, the “Centro di Ricerca per la Frutticoltura” in Rome has developed a crossbreed from different species of *A. deliciosa*, called Cl.GI cultivar, to obtain kiwifruits characterized by an earlier ripening than that of Hayward kiwifruits. In this way, it would be possible to have mature fruits even when Hayward kiwifruits are still unripe, thus promoting the marketing of the product also in this period. Among other *Actinidia* species, Hort16A kiwifruit from *Actinidia chinensis*, marketed under the name of Zespri Gold kiwifruits, hereafter referred to simply as Zespri, has assumed a certain commercial relevance being characterized by a yellow flesh and a flavor sweeter than that of Hayward kiwifruit. These fruits are the only *A. chinensis* kiwifruits produced outside China. They sprout a few weeks in advance of the cultivar

Hayward and bloom about a month before Hayward, and the ripening is usually 1 month earlier than that of Hayward.

Recently, in Italy, a bacterial canker, originally observed in Japan in 1989,² has severely affected kiwifruit orchards, particularly Zespri, causing a serious economic loss for the country, including the impact on trade. The disease is seriously threatening to wipe out Zespri kiwifruit orchards in Italy. Knowledge of the mechanisms responsible for resistance to infections and diseases is mandatory for strategies to be defined that may improve resistance in highly susceptible crop species. With the progress of genomic initiatives to profile genome and gene expression, metabolic profiling is increasingly needed for a better understanding of plant defense mechanisms. Metabolic profiling may also help in discriminating various cultivars, in investigating nutritional properties, processing, and shelf life, in monitoring the development of the fruit, and in assessing the proper harvesting time. Nuclear magnetic resonance plays an important role as it yields a comprehensive metabolic profile and also provides direct structural information regarding individual metabolites in the mixture.

Special Issue: IX Italian Congress of Food Chemistry

Received: July 4, 2012

Revised: October 17, 2012

Accepted: October 19, 2012

Published: October 19, 2012

Various analytical approaches focused on specific class of compounds (target analysis) have been used to investigate kiwifruit nutritional properties³ and sensory characteristics and processing.⁴ Moreover, in a previous paper,⁵ the metabolic profiling of Hayward kiwifruit aqueous extracts and the water state of entire kiwifruits have been monitored over the season using NMR methodologies. The metabolic profiling of aqueous kiwifruit extracts has been investigated by means of high-field NMR spectroscopy, whereas the water state of the entire fruit has been monitored in a noninvasively way directly on the intact fruit by means of a portable unilateral NMR instrument.⁶ In this paper, the methodology previously proposed to study Hayward kiwifruits was applied to study kiwifruits of CIGI and Zespri cultivars. A comparison among the results obtained for three cultivars is reported. An improvement of the spectral assignment of kiwifruit aqueous extracts was achieved using 2D experiments and spiking experiments.

Preliminary results obtained with portable NMR directly in field on the fruits attached to the tree are also reported.

MATERIALS AND METHODS

Materials. Zespri, Hayward, and CIGI kiwifruits were hand harvested in an experimental field located in Lazio district, Italy. These three varieties were purposely chosen because they have different developmental times; in fact, Zespri fruits are usually about 1 month earlier than Hayward fruits, whereas the developmental time of CIGI fruit is intermediate between Zespri and Hayward.

In this orchard the agronomic conditions were identical. Plants of the collection were 10 years old, grafted on D1 Vitroplant rootstock, spaced at 4 × 5 m, and trained to a pergola trellis. A drip irrigation system guaranteed regular availability of water.

To monitor many stages of kiwifruit development, fruits were analyzed over the season from June 2008 (60 days after anthesis⁷) to December 2008 and before reaching the eating-ripe stage.

Low-field NMR measurements were carried out on intact kiwifruits immediately after harvest. Subsequently, the same kiwifruits were subjected to an extraction procedure and used for high-field NMR analysis.

Low-field NMR measurements were also carried out on intact kiwifruits still attached to the plant. Measurement were performed in the field in October, November, and December.

Sample Preparation. Fresh cut pulp (1 g) was frozen in liquid N₂, finely powdered, and submitted to an extraction according to the modified⁸ Bligh–Dyer methodology⁹ with methanol/chloroform/water in 2:2:1 volumetric ratio. Sample was kept at 4 °C for 1 h and then centrifuged for 20 min at 11000g at 4 °C. The upper hydroalcoholic phase and the lower organic phase were separated and dried under an N₂ flow. The dried phases were stored at –80 °C until the NMR analysis.

NMR Spectroscopy. The dry residue of the hydroalcoholic phase was dissolved in a D₂O phosphate buffer (100 mM, pH 7.2) containing 3-(trimethylsilyl)propionic-2,2,3,3-*d*₄ acid sodium salt (TSP, 2 mM). TSP was used both as chemical shift reference and as relative intensity standard.

The NMR spectra of kiwifruit aqueous extracts were recorded at 27 °C on a Bruker AVANCE 600 spectrometer operating at the proton frequency of 600.13 MHz and equipped with a Bruker multinuclear z-gradient inverse probehead. ¹H spectra were referenced to TSP signal ($\delta = 0.00$ ppm), whereas ¹³C spectra were referenced to the CH-1 resonance of α -D-glucose ($\delta = 93.10$ ppm).

The ¹H spectra of aqueous extracts were acquired by co-adding 512 transients with a recycle delay of 3 s, an acquisition time of 2.3 s, using a 60° pulse of 7.3 μ s, and 32K data points.

The chosen recycle time value allowed us to achieve an adequate signal-to-noise ratio in the spectrum in a feasible total acquisition time. Taking into account that the *T*₁ value for different metabolites in the aqueous extract is in the range of 0.5–3 s, the experimental parameters

were not sufficient to achieve a complete relaxation of slowly relaxing nuclei; nevertheless, a comparison between samples is still possible because each spin undergoes the same relaxation phenomenon.

To minimize the variability of the signal intensity due to water suppression, a simple solvent presaturation pulse sequence, in which a soft pulse, corresponding to an excitation window of about 6 Hz, centered at the offset frequency, was applied during the relaxation delay. Moreover, the offset calibration was performed in each spectrum to minimize residual HDO signal.

2D NMR experiments, namely, ¹H–¹H COSY, ¹H–¹H TOCSY, ¹H–¹H NOESY, ¹H–¹³C HSQC, and ¹H–¹³C HMBC,¹⁰ were performed using the same experimental conditions previously reported.¹¹ The mixing time for ¹H–¹H TOCSY was 80 ms, and the mixing time for ¹H–¹H NOESY was 400 ms. HSQC experiments were performed using a coupling constant ¹J_{C–H} of 150 Hz, and ¹H–¹³C HMBC experiments were performed using a delay of 80 ms for the evolution of long-range couplings.

Pulsed field gradient spin echo experiments^{12,13} were performed with a pulsed field gradient unit producing a magnetic field gradient in the z-direction with a strength of 55.4 G cm^{–1}. The stimulated echo pulse sequence using bipolar gradients with a longitudinal eddy current delay was used. The strength of the sine-shaped gradient pulse with a duration of 1.4 ms was incremented in 32 steps, from 2 to 95% of the maximum gradient strength, with a diffusion time of 120 ms and a longitudinal eddy current delay of 25 ms. After Fourier transformation and a baseline correction, the diffusion dimension was processed using the DOSY^{14,15} subroutine of the Bruker TOPSPIN 1.3 software package.

The correction of baseline was applied before the measurement of the intensity. Baseline correction was carried out using a set of points distributed over the ¹H spectrum using a baseline correction routine in TOPSPIN Bruker software.

Statistical Analysis. The intensity of selected ¹H resonances for water-soluble metabolites⁴ (see Table 2) was measured with respect to the intensity of TSP. The intensity of the TSP signal was stable in steady-state conditions. To perform a comparison between ¹H spectra of kiwifruits from different varieties, the signal line width of each specific resonance has to be the same in all analyzed spectra. It can be obtained by using the same experimental protocol including sample preparation, acquisition, and processing procedures for all samples. Under these conditions, the intensity (height of the resonance) as well as the integral is proportional to the molar concentration. Because the measurement of the intensity is much less affected by peaks overlapping with respect to the integral measurement, in the present work the peak intensity was used for the statistical analysis.

The statistical processing of NMR data was carried out using Unscrambler 9.8 software (CAMO Software, Oslo, Norway). To analyze the multivariate structure of the data principal component analysis (PCA) and partial least squares regression (PLS) were applied to the intensity of ¹H selected resonances (see Table 2). The data matrix was pretreated by autoscaling: the means of each column were set to 0, whereas their standard deviations were set to 1.¹⁶ This procedure, applied to the data matrix prior to PCA or PLS analyses, allows comparison of the covariations of the signals independent of their numerical size, keeping intact the factorial structure.

PLS2 is a straightforward extension of the standard PLS analysis, where the array of values of the external variable, along which the multivariate regression is performed, is substituted by a matrix of two (or more) external variables, in our case, the stage of kiwifruit development and kiwifruit cultivar. PLS2 gives no better predictive results than PLS, but it is more suitable in the presence of interactions between the external variables. The analysis results in a single set of scores, a single set of loadings, and separate sets of correlation coefficients for each external variable.¹⁷

¹H Low-Field Measurements Using Portable Unilateral NMR. All measurements were carried out using a portable unilateral NMR instrument from Bruker Biospin. The probehead of the instrument is made of a U-shaped magnet assembled with two permanent magnets mounted on an iron yoke and including a radio frequency resonator.^{18,19}

Table 1. Assignment of New Compounds Identified in the ^1H Spectrum of Aqueous Extract of Kiwifruit

| compound | assignment | ^1H (ppm) | multiplicity (Hz) | ^{13}C (ppm) |
|--|---|--------------------|-------------------|-----------------------|
| phenylalanine (PHE) | $\alpha\text{-CH}$ | 4.000 | dd | |
| | $\text{CH}_2 \beta, \beta'$ | 3.292, 3.1389 | dd, dd | 37.38 |
| | CH-2,6, ring | 7.336 | m | 130.50 |
| | CH-3,5, ring | 7.436 | m | 130.20 |
| | CH-4, ring | 7.384 | m | 128.72 |
| histidine (HIS) | $\text{CH}_2 \beta, \beta'$ | 3.364 | dd (7.2, 4.1) | |
| | CH-2, ring | 8.679 | d (1.4) | |
| | CH-4, ring | 7.405 | d (1.4) | |
| | CH-6' | 6.957 | | |
| 3-O- α -L-rhamnopyranosyl quercetin (Q-RAM) | CH-6 | 6.369 | d (2) | 100.14 |
| | CH-8 | 6.569 | d (2) | 95.74 |
| | CH-2' | 7.371 | d (2) | 117.53 |
| | CH-5' | 7.065 | d (8) | 117.09 |
| | CH-6' | 7.341 | dd (2,8) | 123.77 |
| | $\text{CH}_3\text{-6}''$ | 0.869 | t (6.2) | 17.24 |
| | CH-5'' | 3.110 | | |
| | CH-4'' | 3.358 | | |
| | CH-3'' | 3.775 | | |
| | CH-2'' | 4.263 | | |
| CH-1'' | 5.256 | d (1.5) | 102.7 | |
| neochlorogenic acid (NCGA) | CH-8 | 6.453 | d (16) | |
| | CH-7 | 7.674 | d (16) | |
| | CH-6 | 7.166 | dd (2,8) | |
| | CH-5 | 6.970 | d (8) | |
| | CH-2 | 7.235 | d (2) | |
| | CH-3' | 5.4146 | | |
| | $\text{CH}_2\text{-2}'/\text{CH}_2\text{-6}'$ | 1.96–2.27 | | |
| epicatechin (EPC) | CH-8 | 6.137 | d (2) | |
| | CH-6 | 6.117 | d (2) | |
| | CH-6' | 7.069 | d (1.4) | |
| | CH-3', CH-2' | $\cong 6.969$ | | |
| | CH-2 | 5.029 | | |
| caffeoyl-R (CAFFR) | CH-2 | 7.254 | d (2) | 116.30 |
| | CH-5 | 6.957 | d (8) | 117.25 |
| | CH-6 | 7.180 | dd (2, 8) | 123.80 |
| | CH-7 | 7.734 | d (16) | 145.42 |
| | CH-8 | 6.498 | d (16) | 115.22 |

The entire kiwifruit was positioned in contact with the probehead. Note that the analyzed fruits were similar in size. The NMR signal was obtained from a sensitive detection region 1 mm thick and centered at a depth of 0.5 cm from the outermost surface of the entire unpeeled kiwifruit. As a consequence, measurements were carried out in the outer pericarp over the season (June–February).

Measurements were performed using a probehead operating at 16 MHz, the 90° pulse width was 10.4 μs , and the recycle delay was 3 s. Because in a nonhomogeneous magnetic field the NMR signal decays quickly, the NMR signal must be recovered stroboscopically.¹⁹ Therefore, the signal intensity or integral is actually the intensity or integral of the signal resulting after application of the Hahn echo pulse sequence.²⁰

Transverse T_2 relaxation times were measured with a CPMG pulse sequence;^{21,22} 2048 echoes were collected using an echo time τ of 150 μs . All kiwifruits were analyzed using the same experimental parameters.

Measurements were carried out from June 2008 to December 2008. Nine kiwifruits from each cultivar were measured during each stage of

development. To investigate the effect of storage, measurements were also carried out in February, after storage at 4 $^\circ\text{C}$ for 2 months.

Additionally, measurements were also carried out directly in the field from October until December on kiwifruits attached to the plant. Twenty kiwifruits from each cultivar were measured at each stage of development.

Processing of Experimental Data from CPMG Pulse Sequence. The decay of the magnetization obtained after application of a CPMG pulse sequence is usually a mono- or multiexponential process.^{23,24} Data are fit to a monoexponential function in the case of a bulk liquid or to a multiexponential function in the case of heterogeneous systems:²⁵

$$M_1 = C_0 + \sum_{j=1}^N W_j \exp\left[-\frac{t}{T_{2j}}\right] \quad (1)$$

N is the number of components to fit the decay, T_{2j} and W_j are the transverse relaxation time and the spin population of the j th component, respectively, and C_0 is an offset value. Usually best fits

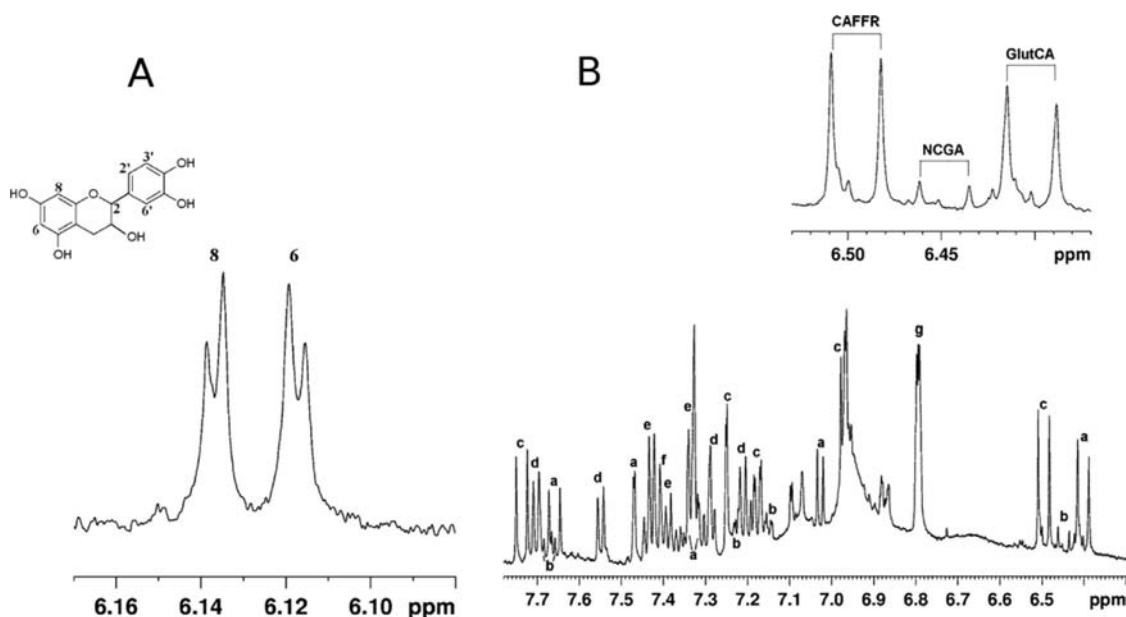


Figure 1. (A) Spectral region of characteristic signals of epicatechin. (B) Aromatic spectral profile of Zespri cultivar at an early stage of development (June) along with resonance assignment: GLUtCA (a); NCGA (b); CAFFR (c); TRP (d); PHE (e); HIS (f); SHA (g). (Inset) Resonances particularly diagnostic for the presence of GLUtCA, NCGA, and CAFFR in expanded scale.

with an increasing number of components are carried out to fit CPMG decays measured in heterogeneous systems. The suitable number of components is the lowest number of components that, according to criteria such as *F* test or correlation factor R^2 , gives a satisfactory best fit of experimental data.

The inhomogeneous magnetic field generated by portable NMR constitutes a further source of relaxation, which shortens T_2 values.^{26–28}

In a first step of work decays obtained were fit to a three-exponential function. However, the shortest T_2 component was found to be ill-defined (error of the order of 20% of the nominal value), as in the CPMG decay only the first few experimental points accounted for this component. Using an echo time as short as possible (40 μ s), it is possible to slightly increase the number of experimental points relative to the shortest T_2 component. However, the echo time was found to be not sufficient to detect the whole longest T_2 component in a single CPMG experiment. For the present measurements, the maximum number of echoes detectable in a single experiment is 2048. Even using the shortest echo time, the shortest component did not show any clear trend with the season. The same finding has been reported in kiwifruits subject to osmotic dehydration,²⁶ where the shortest T_2 component has been reported to be rather unaffected by the treatment. We decided to disregard the shortest component, removing the first experimental points from the CPMG decay. According to this choice experimental data were fit to a biexponential function, and the two components obtained were labeled “a” and “b”, respectively. Best fits, with a correlation factor R^2 of better than 0.998, were accepted.

A regularized inverse Laplace transformation²⁹ was applied to invert the CPMG decay using a software implemented within the Matlab (MathWorks) framework. After the transformation, data were represented as a distribution of relaxation times. In this representation, the maxima (peaks) of the distribution are centered at the corresponding most probable T_2 values, whereas peak areas correspond to the relative spin populations.

RESULTS AND DISCUSSION

Additional ^1H NMR Spectral Assignment. The assignment of the ^1H spectrum of kiwifruit aqueous extract has been reported in a previous paper.⁵

In the present paper, a refined assignment was obtained using 2D experiments and spiking experiments. In particular, histidine

(HIS), phenylalanine (PHE), and epicatechin (EPC) were identified in Zespri, Cl.GI, and Hayward aqueous extracts. A quercetin derivative, namely, 3-*O*- α -L-rhamnopyranosyl quercetin (Q-RAM), was identified only in Cl.GI and Hayward aqueous extracts, whereas neochlorogenic acid (NCGA) was detected only in Zespri extracts. HIS and PHE were identified by means of their characteristic ^1H chemical shifts (see Table 1). EPC (see the sketch in Figure 1) was identified in the ^1H spectrum by means of the characteristic aromatic signals at 6.117 (CH-6) and 6.137 ppm (CH-8) (see Figure 1A). The assignment of the other aromatic protons at 7.069 ppm (CH-6') and 6.969 ppm (CH-3' and CH-2') and of CH-2 at 5.029 ppm was confirmed by the addition of the corresponding standard compound.

Another compound with a caffeoyl moiety, here reported as caffeoyl-R (CAFFR), was also partially assigned (see Table 1 and peaks labeled with “c” in Figure 1B). Protons of the caffeoyl moiety were assigned by TOCSY experiment. Important information regarding the molecular weight of the investigated compound was obtained by DOSY experiment.^{14,15} DOSY is a particularly convenient way of displaying the molecular self-diffusion information in a bidimensional array, with the NMR spectrum in one dimension and the self-diffusion coefficient in the other one. DOSY has been also proposed as a versatile tool for achieving a simple estimation of the molecular weight of uncharged compounds in dilute aqueous solutions.³⁰ In the case of CAFFR, the DOSY experiment indicated a molecular weight of about 360 Da, suggesting the presence of a substituent R in the caffeoyl moiety. However, the absence of NOE contacts excludes the presence of substitution in positions 3 and/or 4 of the aromatic ring. Although it was not possible to assign completely this compound, the assignment of this structure to chlorogenic acid and/or its isomers was excluded by spiking experiments.

Q-RAM (see the sketch in Figure 2) was identified in the ^1H spectrum of Cl.GI and Hayward kiwifruit aqueous extracts by means of 2D experiments. The 6.30–7.45 ppm spectral region reported in Figure 2A shows the assignment of the aromatic

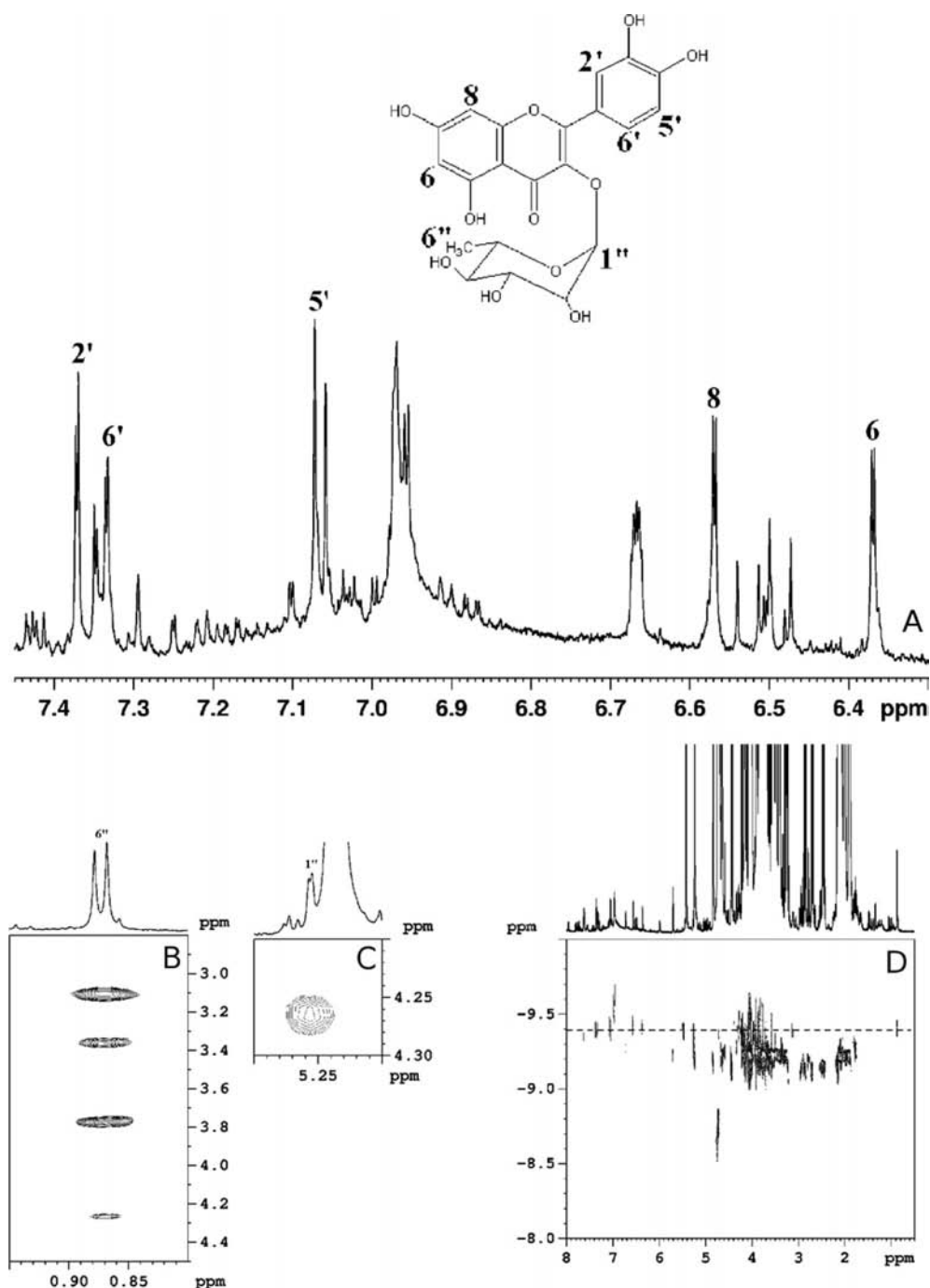


Figure 2. (A) Typical aromatic spectral region of CLGI and Hayward kiwifruit aqueous extract. The assignment of the aromatic moiety of 3-O- α -L-rhamnopyranosyl quercetin (Q-RAM) (sketch) is also reported. (B, C) Expansions of ^1H - ^1H TOCSY map: the spin system of rhamnosyl moiety was completely identified by means of CH-1'' and CH-6'' cross-peaks. (D) DOSY map of CLGI kiwifruit aqueous extract.

protons obtained by TOCSY experiment. The rhamnosyl moiety was also identified by means of the TOCSY experiment, which allowed the identification of the corresponding spin system; in fact, CH₃-6'' correlates with protons at 3.110, 3.358, 3.775, and 4.263 ppm due to CH-5'', CH-4'', CH-3'', and CH-2'', respectively, whereas CH-1'' at 5.256 ppm shows a clear correlation with proton at 4.263 ppm due to CH-2'' (see Figure 2B,C). The DOSY map clearly demonstrated that the aromatic rings and the rhamnosyl moiety belong to the same molecule, as they displayed the same self-diffusion coefficient (see Figure 2D).

In the literature EPC, Q-RAM, and *O*³- β -glucopyranosylcaffeic acid (GLUcA) have been also detected by chemical fractionation of pulp crude extract from Hayward kiwifruit³¹ and characterized by reversed-phase HPLC.³²

In Zespri aqueous extracts, NCGA was also identified by means of the characteristic spin system (see peaks labeled "b" in Figure 1B) and by the addition of the corresponding standard compound. All protons belonging to the caffeoyl moiety were assigned, and CH-3', CH-2', and CH-6' of the quinic moiety were also identified (see Table 1).

The crowded aromatic region of an aqueous Zespri kiwifruit extract in an early stage of development is shown in Figure 1B

with the labeling of some resonances of GLUcA (a), NCGA (b), CAFFR (c), TRP (d), PHE (e), HIS (f), and SHA (g). The spectral region reported in the inset was found to be particularly diagnostic for the presence of GLUcA, NCGA, and CAFFR.

Metabolic Profiling of Cl.GI and Zespri Kiwifruits over the Season. To monitor the seasonal variation in the metabolite profile of Cl.GI and Zespri, the intensities of 43 metabolites (see Table 2) were determined and subjected to principal components analysis (PCA). Figure 3A shows the PCA plot of sample scores (PC1 versus PC2) of Cl.GI kiwifruits. These first two PCs account for 56% of the variability within the data, PC1 providing for 31% and PC2 for 25%. In

agreement with the results reported in the case of Hayward kiwifruits,⁴ the effect of the developmental stage is visible as a trend along PC1. Samples collected from June to August are grouped according to the harvesting time along PC1 and PC2. The contribution of the variables to this grouping is given by the variable loadings reported in Figure 3B. GLN, ARG, SHA, URI, and Q-RAM, present in the highest concentration in the first months, and SUCR, GLC, bFRU_{py}, b-GAL, MA, CA, CHN, U7, and U2, present in the highest concentration in the last months, mostly contribute to PC1 and are responsible for the grouping according to the stage of development. In agreement with the maturation process during which the starch hydrolysis occurs, an increase of mono- and disaccharides is observed over the season. As expected, SHA was found to be more abundant at early stages of development as it is a precursor of aromatic amino acids such as PHE and TRP.

Figure 3C shows a PCA plot of sample scores (PC1 versus PC2) of Zespri kiwifruits. These first two PCs account for 52.5% of the variability within the data, PC1 providing for 33.5% and PC2 for 19.0%. PC1 provides mostly the discrimination of kiwifruits according to season. Samples collected in June, July, and August were well grouped according to harvesting time and separated mainly along PC2. Samples collected in September and October appeared separated according to harvesting time along PC1, whereas samples collected later over the season appeared partially overlapped. The contribution of the variables to this grouping was given by the variable loadings reported in Figure 3D. SHA, MI, TRP, and GLN, present in the highest concentration in the first period, and GLC, SUCR, bFRU_{py}, b-GAL, and U5, present in the highest concentration in the last months, were mainly responsible for the grouping according to the stage of development.

Comparison between Cultivars. The metabolic profiling of Zespri, Cl.GI, and Hayward kiwifruits displayed common metabolic features, such as high levels of quinic, citric, and ascorbic acid, but also important differences in the metabolic behavior during the growth and development of fruits (see Figure 4).

In Hayward and Cl.GI the highest concentration of some amino acids such as ARG and GLN was found in the early stages of development and then a decrease was observed (see, for instance, the histogram of ARG in Figure 4). A very different trend was found in Zespri; in fact, ARG increased over the season and the concentration of GLN was rather constant until September, when it decreased (see Figure 4). The concentrations of ARG, GLN, THR, ASN, and ALA were found to be higher in Zespri than in Hayward and Cl.GI. In all three cultivars TRP was present in a similar concentration, the highest being found at early stages of development and then it slightly decreased over the season (data not shown). The level of HIS was found to be higher in Zespri than in Cl.GI and Hayward kiwifruits over the season (see Figure 4). From July until October also the level of PHE was found to be higher in Zespri than in Cl.GI and Hayward kiwifruits. In Hayward and Cl.GI the highest PHE concentration was found at the early stage of development, whereas in Zespri the highest concentration was found from August until October (see Figure 4).

As expected, in the three cultivars, the content of some sugars increased during fruit growth, reaching the highest value in December (see, for instance, the histogram of SUCR in Figure 4). In Hayward kiwifruits, GAL started being detectable

Table 2. Metabolites Used in Statistical Analyses

| metabolite | ¹ H chemical shift, ppm |
|---|------------------------------------|
| 3-O- α -L-rhamnopyranosyl quercetin (Q-RAM) ^a | 0.88 |
| leucine (LEU) | 0.96 |
| valine (VAL) | 0.99 |
| isoleucine (ILE) | 1.03 |
| threonine (THR) | 1.33 |
| lactic acid (LA) | 1.37 |
| alanine (ALA) | 1.49 |
| arginine (ARG) | 1.66 |
| glutamine (GLN) | 2.48 |
| glutamate (GLU) | 2.52 |
| malic acid (MA) | 4.39 |
| citric acid (CA) | 2.73 |
| asparagine (ASN) | 2.97 |
| choline (CHN) | 3.20 |
| myo-inositol (MI) | 3.30 |
| fructose (bFRU _{py}) | 3.58 |
| quinic acid (QA) | 4.17 |
| β -galactose (b-GAL) | 4.60 |
| β -glucose (b-GLC) | 4.67 |
| ascorbic acid (AA) | 4.75 |
| galactose-U (GAL-U) | 5.16 |
| α -glucose (α -GLC) | 5.25 |
| sucrose (SUCR) | 5.42 |
| O ³ - β -D-glucopyranosyl- <i>cis</i> -caffeic acid (GLUcCA) | 5.96 |
| epicatechin (EPC) | 6.13 |
| O ³ - β -D-glucopyranosyl- <i>trans</i> -caffeic acid (GLUtCA) | 6.41 |
| neochlorogenic acid (NCGA) ^b | 6.47 |
| CAFFR | 6.49 |
| shikimic acid (SHA) | 6.68 |
| phenylalanine (PHE) | 7.43 |
| tryptophan (TRP) | 7.55 |
| uridine (URI) | 7.98 |
| adenosine triphosphate (ATP) | 8.58 |
| histidine (HIS) | 8.68 |
| U2 | 1.29 |
| U5 | 5.51 |
| U6 | 5.69 |
| U7 | 5.89 |
| U14 | 7.08 |
| U16 | 7.11 |
| U20 | 5.32 |
| U21 | 5.58 |
| U23 | 6.53 |

^aPresent only in Hayward and Cl.GI kiwifruits. ^bPresent only in Zespri kiwifruits.

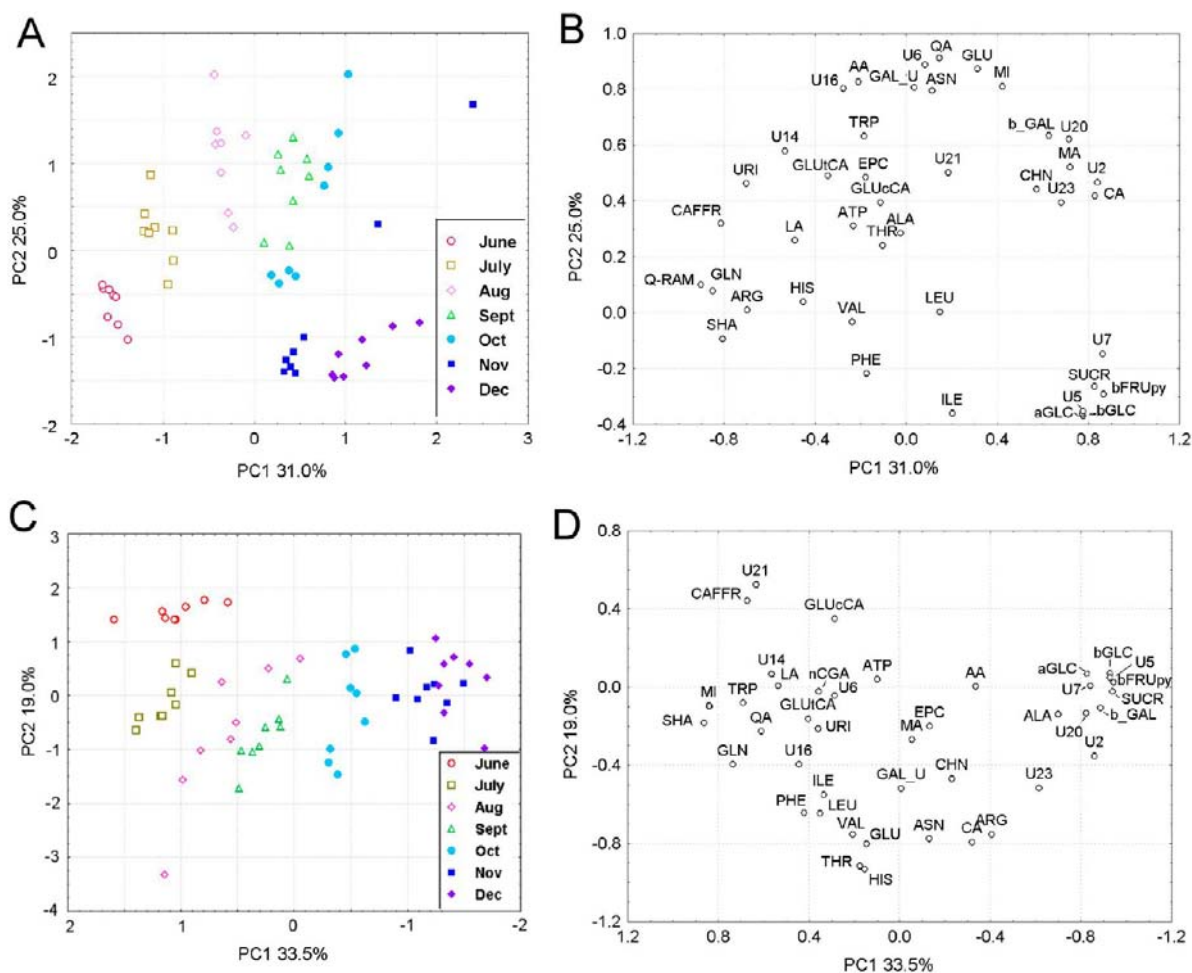


Figure 3. PCA applied to the intensity of 43 ^1H resonances monitored over the season in CI.GI (A, B) and Zespri samples (C, D): (A, C) plot of PC scores; (B, D) plot of variable loadings.

in August, then decreased until October, and then increased again. In CI.GI this compound was already detectable in June, reached the highest concentration in September, and then decreased again. In Zespri the amount of GAL monotonically increased from June to December (see Figure 4). In all three cultivars, MI showed a concentration increase between June and August followed by a decrease at a later stage of development (see Figure 4).

According to the literature,³³ fruits from *Actinidia* species have a relatively high total acid content (1–3% w/w) with quinic and citric acid between 40 and 60% and malic acid about 10%. Quinic acid represents a higher proportion of the total acids during early fruit development.³⁴ In all three cultivars, we found a wide concentration difference between QA and SHA, the average concentration of QA being about 2 orders of magnitude higher than that of SHA (see Figure 5). Moreover, in Hayward and CI.GI SHA disappeared at stages of development later than July. Quinic acid is a key intermediate in lignin biosynthesis, folic acid metabolism, aromatic acid synthesis, anthranilate biosynthesis, and purine metabolism. Shikimic acid is an intermediate of this phenylpropanoid pathway, but in *Actinidia* species its concentration was found to be lower than that of quinic acid. The molecular and enzymatic control of quinic acid storage and metabolism is poorly known, but the enzyme quinate dehydrogenase/shikimate dehydrogenase (EC 1.1.99.25) has been recently suggested³³ to be involved

in the synthesis of quinate and shikimate, through the production of NADP⁺ or NADPH, respectively. The high concentration of quinic acid we found in *Actinidia* species might suggest a balance between the accumulation and consumption of this intermediate, in the early step of development, to ensure a flux of intermediates of phenylpropanoid pathway and NADPH in the last final steps of maturation. This behavior appears to be confirmed by the decreasing trend of SHA over the season. A weak decrease of the level of QA was also observed at late stages of development (see Figure 5). It has been shown that quinic acid, as a constituent of diet, is transformed to tryptophan and nicotinamide via gastrointestinal tract microflora, thus providing an in situ physiological source of these essential metabolic ingredients to humans.³⁵ The co-metabolites produced by the phenylpropanoid intermediate metabolism and excreted by urine can be considered as biomarkers of the host/gut microbiota interaction.³⁶

An increased production of phenolic compounds and flavonoids has been related to reduced susceptibility or increased resistance to fungal or microbial infection in immature fruits.³⁷ In the literature differences in transcripts and metabolites detected in grapevine cultivars have been discussed in terms of metabolic pathways and their possible role in plant defense against pathogen attack.³⁸ In this context, a relevant amount of *O*³- β -D-glucopyranosyl-*trans*-caffeic acid

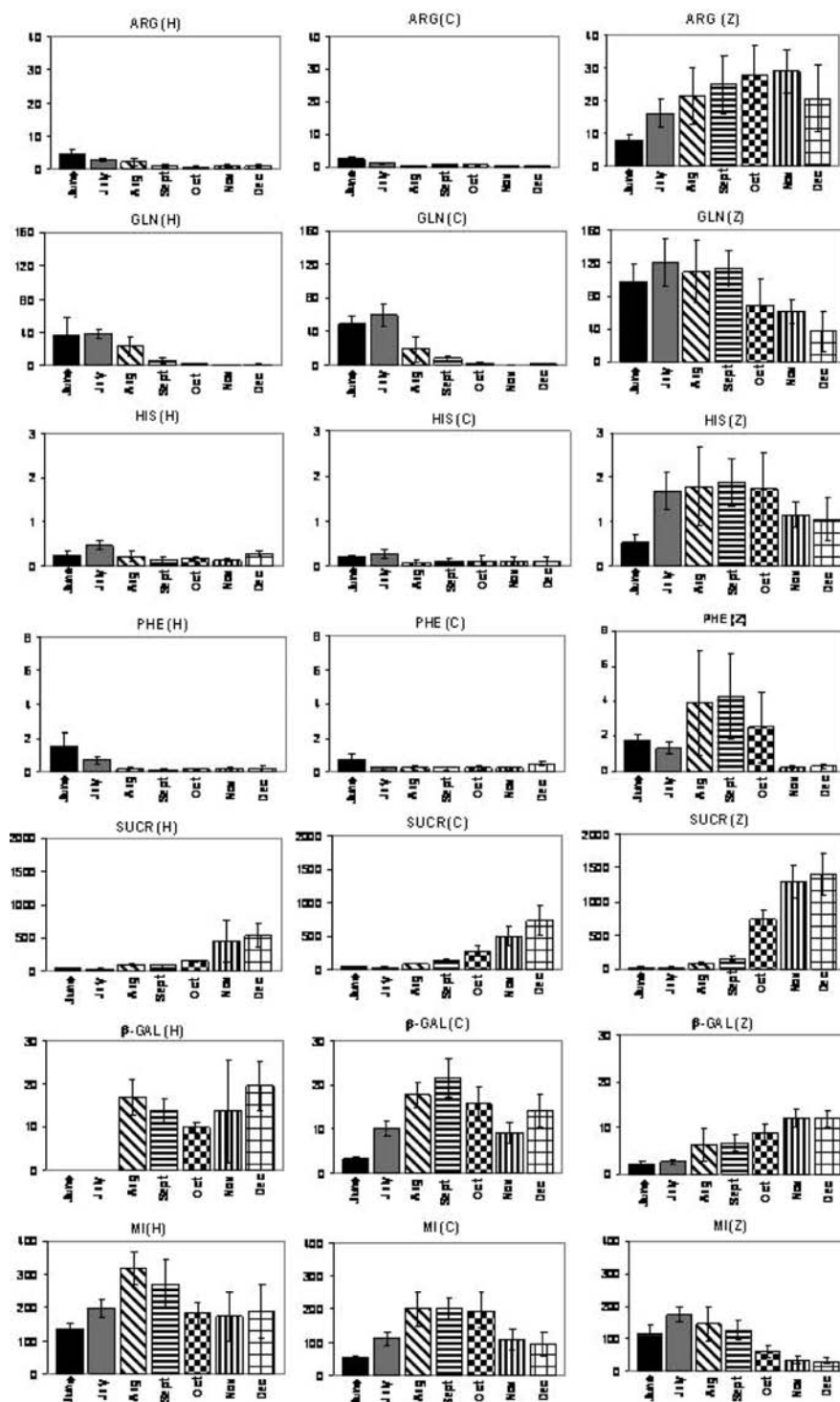


Figure 4. Histograms of some amino acids and sugars resulting from the quantitative NMR spectroscopic analysis of selected resonances present in aqueous extracts of Hayward (H), Cligi (C), and Zespri (Z) kiwifruits. The relative molecular abundance is reported versus the developmental stage. Data shown are the mean \pm SD.

(GLU_tCA) was found to be higher in immature Hayward and Cligi kiwifruits than in Zespri (see Figure 5). Furthermore, Hayward and Cligi immature kiwifruits showed the presence of a phenolic compound, namely, 3-*O*- α -L-rhamnopyranosyl quercetin (Q-RAM), that was absent in the Zespri cultivar (see Figure 5). Vice versa, Zespri kiwifruits displayed the presence of neochlorogenic acid (NCGA), which can be considered a specific marker of this variety, but at a lower level with respect

to other phenolic compounds present in Hayward and Cligi. In Hayward and Cligi kiwifruits, also a significant amount of epicatechin (EPC) was detected in August, whereas in Zespri the amount of this compound was found to be low over the season (see Figure 5).

Figure 6A displays the mean and standard deviation PCA scores at each stage of development relative to the first two principal components obtained on the whole data matrix. The

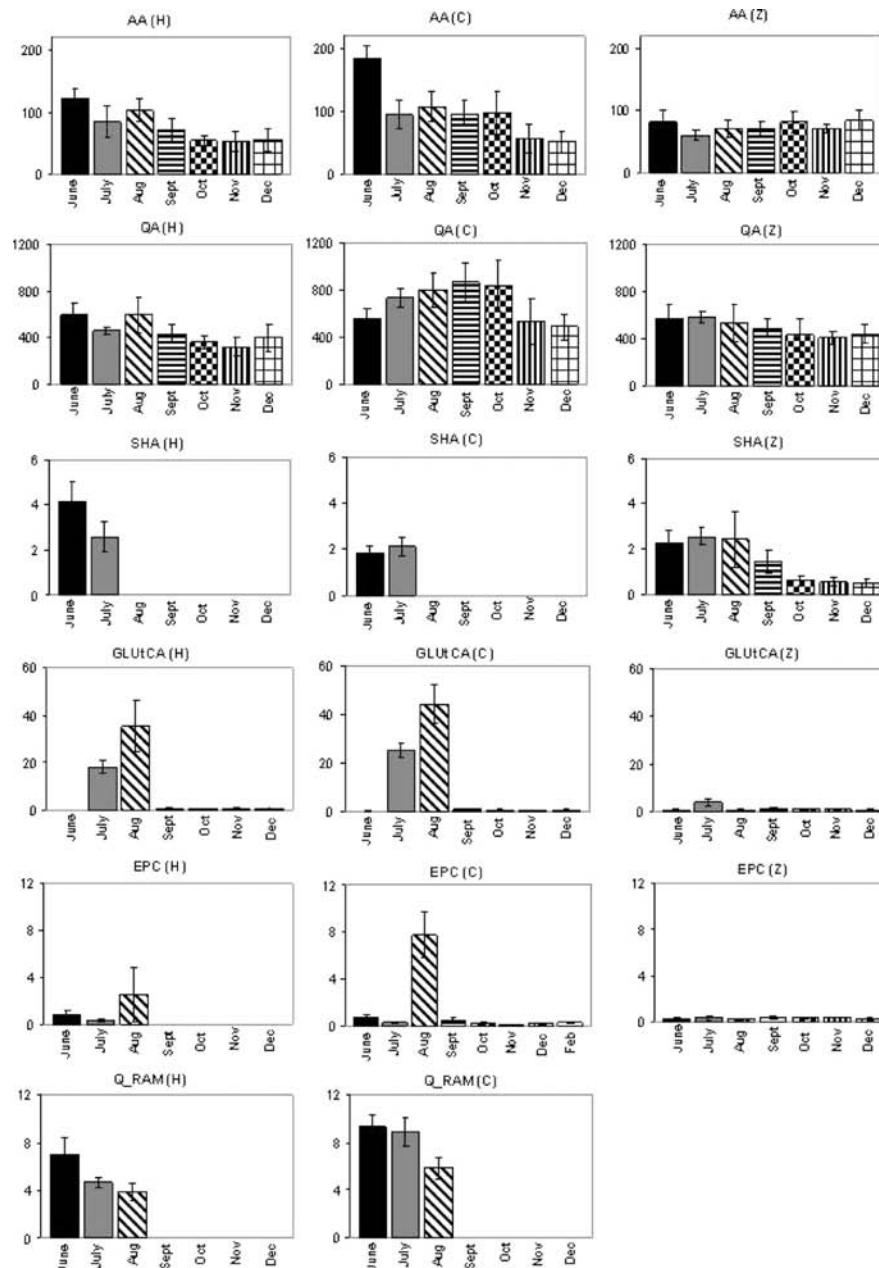


Figure 5. Histograms of some organic acids, phenolic acids, and flavonoids resulting from the quantitative NMR spectroscopic analysis of selected resonances present in aqueous extracts of Hayward (H), Cligi (C), and Zespri (Z) kiwifruits. The relative molecular abundance is reported versus the developmental stage. Data shown are the mean \pm SD.

first principal component is related to the developmental stage of the fruit, whereas the second one is related to the cultivar. By observing the evolution of the scores along PC1, it can be seen that Zespri metabolic profiles always preceded their Hayward and Cligi counterparts, thus confirming the Zespri attitude to an earlier ripening. Hayward and Cligi profiles were substantially coupled along the first as well as the second component. This is confirmed by a PCA carried out only on the Hayward and Cligi profiles, which resulted in no significant separation between the two cultivars (data not shown). This finding is in agreement with the common origin of Cligi and Hayward as they are both varieties of *A. deliciosa*. To single out the effect of the season over the metabolic profiles of the three cultivars, PCA was led on metabolites common to all cultivars at each developmental stage. As an example, the results of three

of such analyses regarding three months, namely, June, August, and December, are reported in Figure 6 and in the Supporting Information. Metabolic profiles of Zespri cultivar were always well separated along PC1 from the other two cultivars at each of the selected months, whereas Hayward and Cligi showed a separation along PC2 only in June (see Figure 6B). In June the separation of Zespri from the remaining was dominated by two groups of amino acids; in fact, ASN, GLN, HIS, TRP, and ARG showed higher levels in Zespri than in Cligi and Hayward, whereas ILE and ALA showed an opposite behavior (see Figure 6C). GLU, PHE, and THR were not significant for this separation. bFRUpy showed a higher level in Zespri than in Cligi and Hayward, whereas SUCR and GLC showed an opposite behavior. Other metabolites such as MA and GLUtCA showed higher levels in Zespri than in the other kiwifruits. The

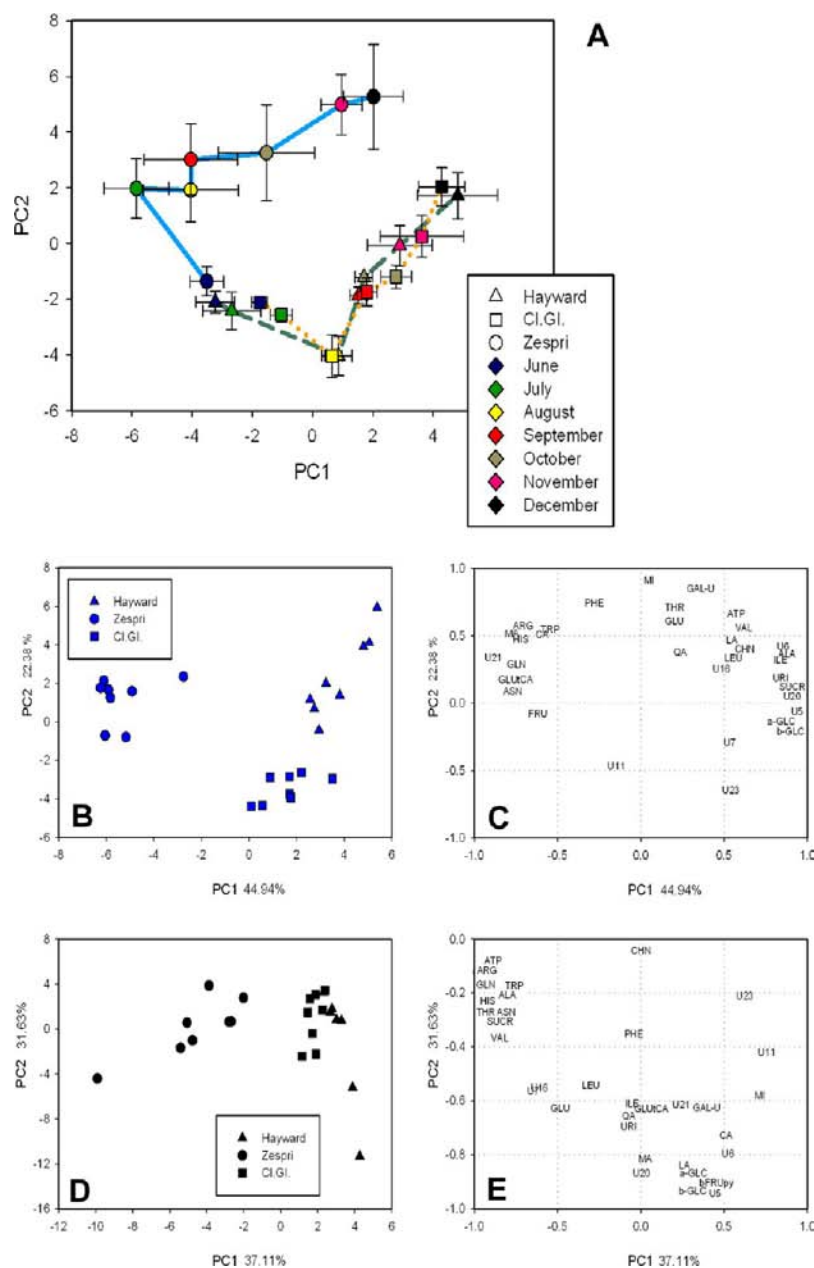


Figure 6. (A) PCA applied to the intensity of selected ^1H resonances (see Table 2), monitored as a function of the developmental stage in Zespri, Cl.GI, and Hayward kiwifruits. Means and standard deviations of the scores are reported. Score plots and loading plots from PCA at different stages of development: June (B, C) and December (D, E). The percentages of the overall variance explained by PC1 and PC2 are shown.

separation between Cl.GI and Hayward along PC2 in June was mainly due to higher levels of MI, GAL-U, ATP, THR, PHE, GLU, and VAL and lower levels of some unassigned metabolites such as U23 in Hayward with respect to Cl.GI (see Figure 6C).

In August (Supporting Information) the separation of Zespri from the other fruits was due to the whole set of amino acids (with the exception of GLU) and to ATP, the levels of which were higher in Zespri than in Hayward and Cl.GI kiwifruits, and generally lower levels of many sugar-related metabolites (GLC, GAL-U, GLUtCA, MI, CAFFR) and some unassigned signals (U5, U6, U7, U20, U23).

In December most of the amino acids, namely, GLN, TRP, ALA, HIS, ASN, THR, and VAL, were responsible for the separation of Zespri from the other fruits, along with ATP and

SUCR, whereas GLC, GAL-U, GLUtCA, and MI still showed a higher level in Hayward and Cl.GI than in Zespri fruits (see Figure 6D,E).

PCA was not able to evidence differences between Cl.GI and Hayward kiwifruits over the season. This might be due to the strong difference occurring between Zespri, on the one hand, and Hayward and Cl.GI, on the other hand. To stress a possible different behavior PLS2 analysis was then carried out on the Hayward and Cl.GI samples (Supporting Information). The same variables of PCA were used in PLS2. The PLS2 model is given by four components significant at the Marten's uncertainty test, characterized by regression coefficients $R^2 = 0.94$ and $Q^2 = 0.92$ along the stage of development and $R^2 = 0.91$ and $Q^2 = 0.88$ with respect to the cultivar.

In agreement with the PCA shown in Figure 6A, the score plot obtained from PLS2 analysis (Supporting Information) showed that, with the exception of June and July, data relative to CLGI and Hayward were not separated along PC1, that is, the stage of development, whereas they were well separated along PC2. The most relevant metabolites responsible for this separation, namely, ARG, CHN, MI, QA, SUCR, URI, and HIS, were indicated by their regression coefficients of the PLS2 model with the cultivar; their statistical significance was assessed through the uncertainty test and ANOVA univariate test (see Table 3). According to the PLS2 findings, CLGI fruits

Table 3. Significant Regression Coefficients of the PLS2 Model Analyzed by Uncertainty Test and ANOVA Univariate Analysis^a

| metabolite | regression coefficient | ANOVA P |
|------------|------------------------|----------|
| ARG | -0.1780 | 0.000142 |
| CHN | 0.2790 | 0.000000 |
| MI | -0.2460 | 0.000001 |
| QA | 0.3420 | 0.000000 |
| SUCR | 0.1110 | 0.036784 |
| URI | -0.1170 | 0.00074 |
| HIS | -0.1230 | 0.000001 |

^aCLGI kiwifruits are compared to Hayward kiwifruits.

are characterized by higher levels of CHN and QA and lower levels of ARG, MI, URI, and HIS with respect to the Hayward

fruits over the entire season, whereas these two cultivars have nearly the same levels of SUCR until August, which then increase more swiftly in CLGI than in the Hayward cultivar.

Water State in Outer Pericarp of Hayward, CLGI, and Zespri Kiwifruits over the Season. In fruits and vegetables the mixing of protons from different pools makes the assignment of relaxation times to particular compartments a difficult task. The extent of averaging depends on the rates of exchange between different intercellular sources, on the intrinsic relaxation times, and on morphology.²⁴ As the exchange affects T_1 more than T_2 , T_2 measurements usually yield more detailed information on the compartmentalized water than T_1 measurements.^{24,25}

In the literature, three T_2 components have been measured in apple, revealing the existence of three main different proton pools.³⁹ More recently, the three T_2 components measured in the outer pericarp of kiwifruit have been assigned to three cellular compartments through a kinetic doping experiment with a paramagnetic aqueous solution.²⁶ The shortest T_2 component has been assigned to protons located in the cell walls, the intermediate one to protons in cytoplasm and extracellular space, and the longest one to protons in vacuole.

It has been previously shown that, in the case of Hayward kiwifruits, T_2 values measured with portable NMR were suitable parameters to monitor the water state of the outer pericarp of the fruit as a function of the developmental stage.⁴ In fact, the tendency toward longer T_2 relaxation times later in the season was found to be consistent with a change in the fruit texture

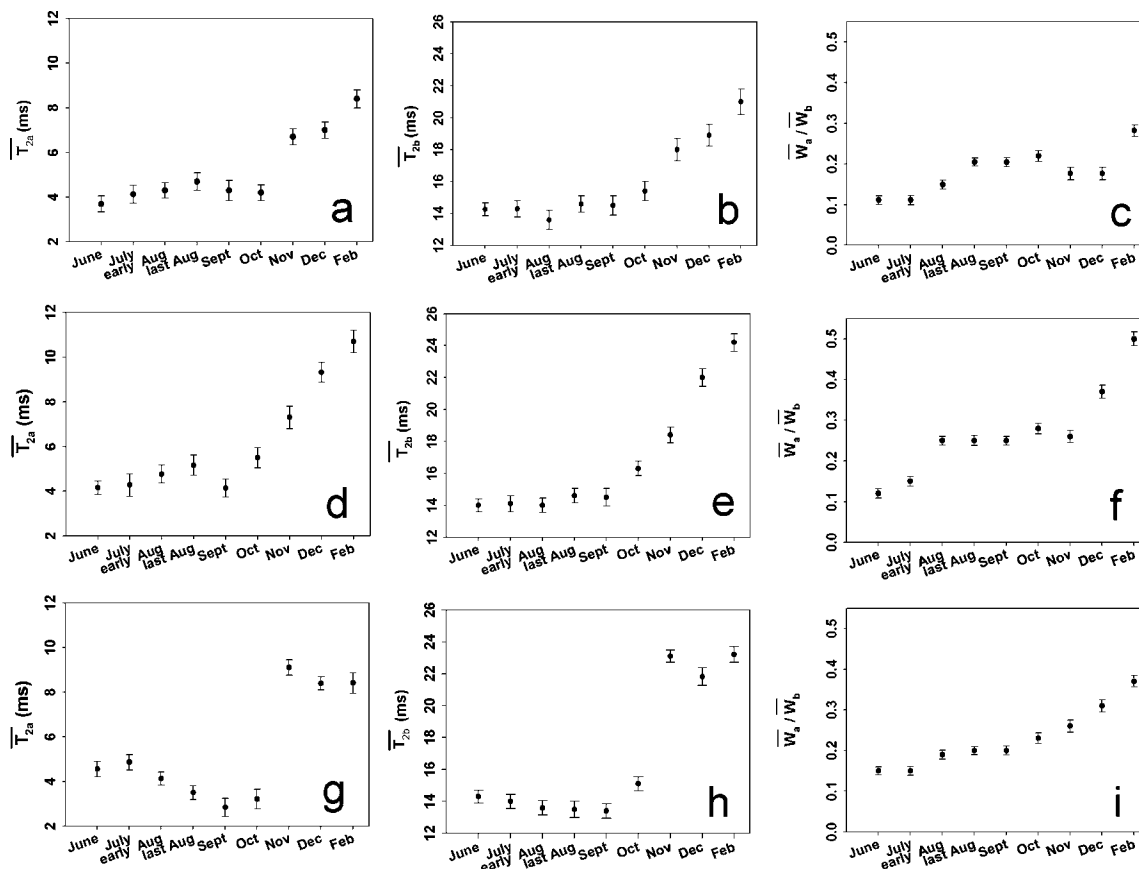


Figure 7. Average T_2 values, T_{2a} and T_{2b} , measured on nine kiwifruits versus the developmental stage of Hayward (a, b), CLGI (d, e), and Zespri (g, h) kiwifruits: W_a/W_b values in Hayward (c), CLGI (f), and Zespri (i) kiwifruits versus the developmental stage. The error bars represent the maximum error calculated with the error propagation theory.

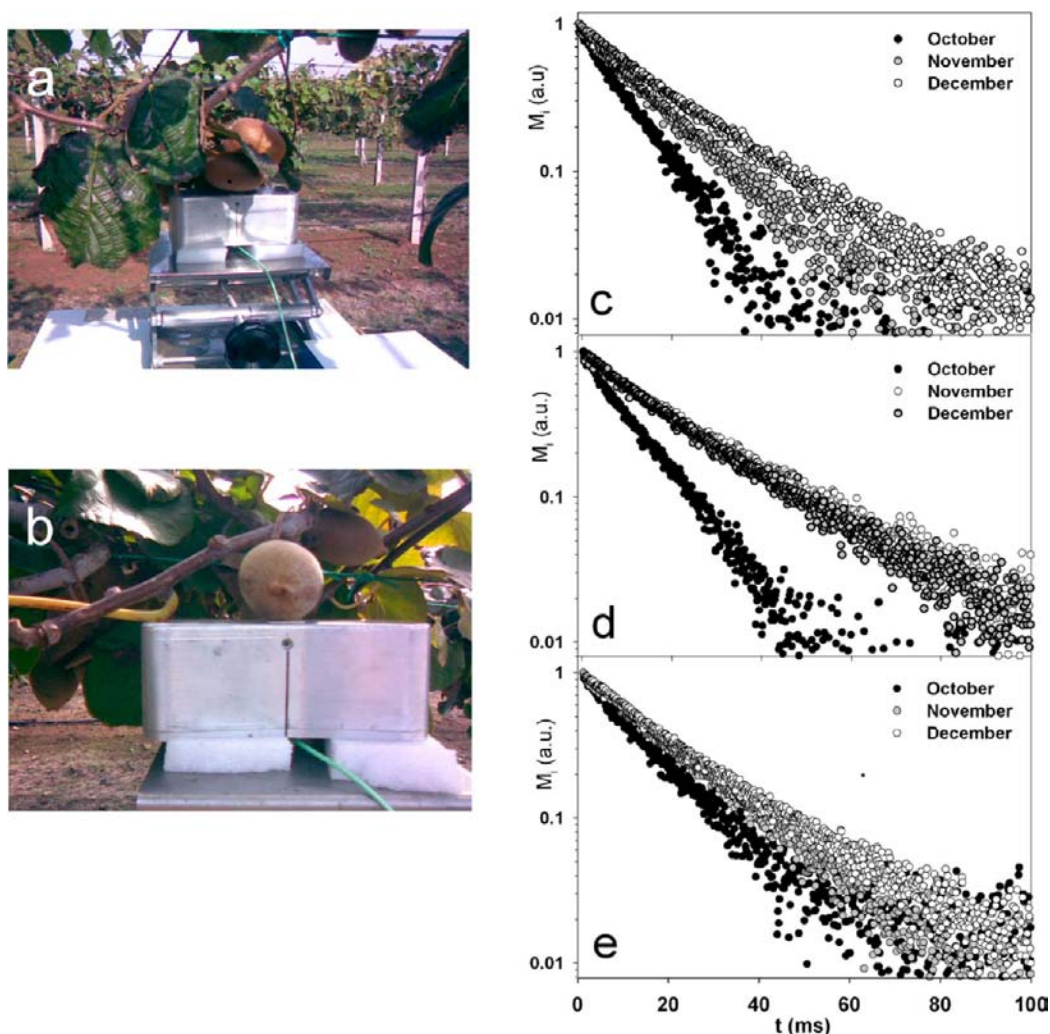


Figure 8. Measurements in field on entire kiwifruits attached to the tree with a portable unilateral NMR instrument (a, b). CPMG decays were measured in October, November, and December on Hayward (c), Zespri (d), and CI.GI (e) kiwifruits (a.u. = arbitrary unit).

occurring during fruit development. The average $\overline{T_{2a}}$ and $\overline{T_{2b}}$ values measured on nine kiwifruits at each stage of development, and ascribed to protons in cytoplasm and extracellular space and to protons in vacuole, respectively, were reported along with the standard deviation (see Figure 7, panels a and b, respectively). The ratio between the average value of spin populations of the two components, namely $\overline{W_a}/\overline{W_b}$, increased from June to September, was constant from September to December, and in February increased again (see Figure 7c). As a result, the spin population ratio increased from 0.11 to 0.28 over the season.

Like Hayward, also in the case of CI.GI and Zespri kiwifruits the CPMG decays measured between June and February were fit to a biexponential function. In CI.GI both $\overline{T_{2a}}$ and $\overline{T_{2b}}$ showed a gradual lengthening between October and February (see Figure 7d,e). The average $\overline{T_{2a}}$ and $\overline{T_{2b}}$ values measured in CI.GI at a time later than November were found to be slightly longer than those measured in Hayward in the same period. $\overline{W_a}/\overline{W_b}$ slightly increased from June to August, and then it remained constant and then increased again (see Figure 7f). From June to February $\overline{W_a}/\overline{W_b}$ increased from 0.12 to 0.50, and both values were greater than those measured in Hayward kiwifruits.

In Zespri a net, sharp lengthening of both $\overline{T_{2a}}$ and $\overline{T_{2b}}$ occurred between October and November (see Figure 7g,h), whereas in Hayward and CI.GI the lengthening was much more gradual (see Figure 7). This behavior possibly accounts for a sharp transition in the Zespri water state, which would be in agreement with the earlier maturation of Zespri with respect to Hayward and CI.GI. At a time later than October, in Zespri both $\overline{T_{2a}}$ and $\overline{T_{2b}}$ were found to be constant, whereas in the same period, relaxation times measured in Hayward and CI.GI progressively increased with the season (see Figure 7). In Zespri $\overline{W_a}/\overline{W_b}$ increased from 0.15 up to 0.37 over the season.

To summarize, in all cases, $\overline{T_{2a}}$ ascribed to proton in cytoplasm and extracellular space and $\overline{T_{2b}}$ ascribed to protons in vacuole lengthened with the season and, contemporary in the former case, the spin population increased with the season, whereas in the latter case it decreased with the season. On average, from October to February, T_2 relaxation times were found to be very sensitive to the kiwifruit developmental stage, whereas constant values were measured at times earlier than October. The ratio between the spin populations was found to be sensitive to the kiwifruit developmental stage over the whole season.

T_2 Relaxation Measurements in Field. The water state of the outer pericarp of Hayward, Zespri, and CI.GI kiwifruits was

also monitored on the entire fruit attached to the plant (see Figure 8a,b). The relaxation time measurements previously carried out on entire, unpeeled, detached fruits allowed us to choose the suitable period of time to follow the kiwifruit development directly in the field. As a consequence, measurements were carried out from October until December on 20 kiwifruits for each cultivar. As an example, CPMG decays measured in October, November, and December are reported in Figure 8, panels c (Hayward), d (Zespri), and e (C.I.GI). According to the kiwifruit developmental stage, in all three cultivars the decays measured in December were much longer than those measured in October. Furthermore, according to the trend observed on detached fruits, in the case of C.I.GI and Hayward kiwifruits a gradual lengthening of CPMG decays measured in the field was observed between October and December, whereas in the case of Zespri the process seemed complete already in November. In fact, decays measured in November and December perfectly overlapped (see Figure 8d). This finding is in agreement with the known earlier maturation of Zespri with respect to Hayward. Finally, in the case of C.I.GI kiwifruits the CPMG decays measured in October were slightly longer than those measured in the other kiwifruits in the same time period (see Figure 8e). This behavior seems to be in agreement with a slight earlier maturation of C.I.GI with respect to Hayward kiwifruits.

■ ASSOCIATED CONTENT

Supporting Information

Additional figures. This material is available free of charge via the Internet at <http://pubs.acs.org>.

■ AUTHOR INFORMATION

Corresponding Author

*Phone: +39 06 90672700. Fax: +39 06 90672477. E-mail: luisa.mannina@uniroma1.it

Notes

The authors declare no competing financial interest.

■ ABBREVIATIONS USED

AA, ascorbic acid; ATP, adenosine triphosphate; ALA, alanine; ARG, arginine; ASN, asparagine; ASP, aspartate; CAFFR, caffeoyl-R; CHN, choline; CA, citric acid; COSY, correlated spectroscopy; CPMG, Carr–Purcell–Meiboom–Gill; DOSY, diffusion ordered spectroscopy; EPC, epicatechin; α FRUfu, α -D-fructofuranose; β FRUfu, β -D-fructofuranose; β FRUpy, β -D-fructopyranose; FRU6P, fructose-6-phosphate; α GAL, α -galactose; β GAL, β -galactose; GAL-U, galactose-U; GARP, globally optimized alternating phase rectangular pulse; GLUtCA, O³- β -D-glucopyranosyl-trans-caffeic acid; GLUcCA, O³- β -D-glucopyranosyl-cis-caffeic acid; α GLC, α -glucose; β GLC, β -glucose; α GLC6P, α -glucose-6-phosphate; β GLC6P, β -glucose-6-phosphate; GLU, glutamate; GLN, glutamine; HMBC, heteronuclear multiple-bond correlation; HSQC, heteronuclear single quantum coherence; ILE, isoleucine; LA, lactic acid; LEU, leucine; LYS, lysine; MA, malic acid; α MAN, α -mannose; β MAN, β -mannose; MI, myo-inositol; NCGA, neochlorogenic acid; NOESY, nuclear Overhauser and exchange spectroscopy; PGSE, pulsed field gradient spin echo; PHE, phenylalanine; QA, quinic acid; Q-RAM, 3-O- α -L-rhamnopyranosyl quercetin; RAF, raffinose; RIB, ribose; SHA, shikimic acid; SUCR, sucrose; THR, threonine; TOCSY, total correlation spectroscopy; TRP, tryptophan; TSP,

trimethylsilylpropionate; URI, uridine; VAL, valine; α XYL, α -xylose; β XYL, β -xylose.

■ REFERENCES

- (1) Ferguson, A. R. New temperate fruits: *Actinidia chinensis* and *Actinidia deliciosa* perspectives on new crops and new uses. In *Perspectives on New Crops and New Uses*; Janick, J., Ed.; ASHS Press: Alexandria, VA, 1999; pp 342–347.
- (2) Takikawa, Y.; Serizawa, S.; Ichikawa, T. *Pseudomonas syringae* pv. *Actinidiae* pv. Nov.: the causal bacterium of canker of kiwifruit in Japan. *Ann. Phytopathol. Soc. Jpn.* **1989**, *55*, 437–444.
- (3) Park, Y. S.; Ham, K.-S.; Kang, S.-G.; Park, Y.-K.; Namiesnik, J.; Leontowicz, H.; Leontowicz, M.; Ezra, A.; Trakhtenberg, S.; Gorinstein, S. Organic and conventional kiwifruit: myths vs. reality, antioxidant, antiproliferative and health effects. *J. Agric. Food Chem.* **2012**, *60*, 6984–6993.
- (4) Mannina, L.; Sobolev, A. P.; Capitani, D. Applications of NMR metabolomics to the study of foodstuffs: truffle, kiwifruit, lettuce, and sea bass. *Electrophoresis* **2012**, *33*, 2290–2313.
- (5) Capitani, D.; Mannina, L.; Proietti, N.; Sobolev, A. P.; Tomassini, A.; Miccheli, A.; Di Cocco, M. E.; Capuani, G.; De Salvador, R.; Delfini, M. Monitoring of metabolic profiling and water state of Hayward kiwifruits by nuclear magnetic resonance. *Talanta* **2010**, *82*, 1826–1838.
- (6) Casanova, F.; Perlo, G.; Blümich, B. Single-sided NMR. In *Single-Sided NMR*; Casanova, F., Perlo, G., Blümich, B., Eds.; Springer-Verlag: Berlin, Germany, 2011; pp 1–7.
- (7) Richardson, A. C.; Bolding, H. L.; McAtee, P. A.; Gunaseelan, K.; Luo, Z.; Atkinson, R. G.; David, K. M.; Burdon, J. N.; Schaffer, R. J. Fruit development of the diploid kiwifruit, *Actinidia chinensis* ‘Hort16a’. *BMC Plant Biol.* **2011**, *11*, 182–96.
- (8) Miccheli, A.; Aureli, T.; Delfini, M.; Di Cocco, M. E.; Viola, P.; Gobetto, R.; Conti, F. Study on influence of inactivation enzyme techniques and extraction procedures on cerebral phosphorylated metabolite levels by ³¹P NMR spectroscopy. *Cell. Mol. Biol.* **1998**, *34*, 591–603.
- (9) Bligh, E. G.; Dyer, W. J. A rapid method of total lipid extraction and purification. *Can. J. Biochem. Physiol.* **1959**, *37*, 911–917.
- (10) Braun, S.; Kalinowski, H.O.; Berger, S. *150 and More Basic NMR Experiments*, 2nd ed.; Wiley-VCH: Weinheim, Germany, 1998; pp 477–517.
- (11) Mannina, L.; Cristinzio, M.; Sobolev, A. P.; Ragni, P.; Segre, A. High-field nuclear magnetic resonance (NMR) study of truffles (*Tuber aestivum vittadini*). *J. Agric. Food Chem.* **2004**, *52*, 7988–7996.
- (12) Morris, K. F.; Stilbs, P.; Johnson, C. S. Analysis of mixtures based on molecular size and hydrophobicity by means of diffusion ordered 2D-NMR. *Anal. Chem.* **1994**, *66*, 211–215.
- (13) Stilbs, P. Fourier transform pulsed-gradient spin-echo studies of molecular diffusion. *Prog. Nucl. Magn. Reson. Spectrosc.* **1987**, *19*, 1–45.
- (14) Morris, K. F.; Johnson, C. S. Diffusion-ordered two-dimensional nuclear magnetic resonance spectroscopy: principles and applications. *J. Am. Chem. Soc.* **1992**, *114*, 3139–3141.
- (15) Johnson, C. S. Diffusion ordered nuclear magnetic resonance spectroscopy: principles and applications. *Prog. Nucl. Magn. Reson. Spectrosc.* **1999**, *34*, 203–256.
- (16) Eriksson, L.; Johansson, L.; Kettaneh-Wold, L.; Trygg, J.; Wikstrom, C.; Wold, S. *Multivariate and Megavariate Data Analysis Basic Principles and Applications (Part I)*; Umetrics AB: Umeå, Sweden, 2006; pp 40–44.
- (17) Brereton, R. G. *Applied Chemometrics for Scientists*; Brereton, R. G., Ed.; Wiley: Chichester, UK, 2007; pp 211–212.
- (18) Eidmann, G.; Savelsberg, R.; Blümmler, P.; Blümich, B. The NMR MOUSE: a mobile universal surface explorer. *J. Magn. Reson. A* **1996**, *122*, 104–109.
- (19) Blümich, B.; Anferova, S.; Kremer, K.; Sharma, S.; Hermann, V.; Segre, A. L. Unilateral NMR for quality control: the NMR-MOUSE®. *Spectroscopy* **2003**, *18*, 18–29.
- (20) Hahn, E. L. Spin echoes. *Phys. Rev.* **1950**, *80*, 580.

- (21) Carr, H. Y.; Purcell, E. M. Effects of diffusion on free precession in nuclear magnetic resonance experiments. *Phys. Rev.* **1954**, *94*, 630–638.
- (22) Meiboom, S.; Gill, D. Modified spin-echo method for measuring nuclear relaxation times. *Rev. Sci. Instrum.* **1958**, *29*, 688–691.
- (23) Farrar, T. C.; Becker, E. D. *Pulse and Fourier Transform NMR*; Academic Press: New York, 1971; pp 22–29.
- (24) Snaar, J. E. M.; Van As, H. Probing water compartments and membrane permeability in plant cells by ^1H NMR relaxation measurements. *Biophys. J.* **1992**, *63*, 1654–1658.
- (25) Watson, A. T.; Chang, C. T. Characterizing porous media with NMR methods. *Prog. Nucl. Magn. Reson. Spectrosc.* **1997**, *31*, 343–386.
- (26) Panarese, V.; Laghi, L.; Pisi, A.; Tylewicz, U.; Dalla Rosa, M.; Rocculi, P. Effect of osmotic dehydration on *Actinidia deliciosa* kiwifruit: a combined NMR and ultrastructural study. *Food Chem.* **2012**, *132*, 1706–1712.
- (27) Tylewicz, U.; Panarese, V.; Laghi, L.; Rocculi, P.; Nowacka, M.; Placucci, G.; Dalla Rosa, M. NMR and DSC water study during osmotic dehydration of *Actinidia deliciosa* and *Actinidia chinensis* kiwifruit. *Food Biophys.* **2011**, *6*, 327–333.
- (28) Santagapita, P.; Laghi, L.; Panarese, V.; Tylewicz, U.; Rocculi, P.; Dalla Rosa, M. Modification of transverse NMR relaxation times and water diffusion coefficients of kiwifruit pericarp tissue subjected to osmotic dehydration. *Food Bioprocess Technol.* **2012**, 1–10.
- (29) Press, W. H.; Teukolsky, W. T.; Vetterling, B. P.; Flannery, B. P. *Numerical Recipes in Chemistry*; Cambridge University Press: Cambridge, UK, 1994.
- (30) Viel, S.; Capitani, D.; Mannina, L.; Segre, A. Diffusion-ordered NMR spectroscopy: a versatile tool for the molecular weight determination of uncharged polysaccharides. *Biomacromolecules* **2003**, *4*, 1843–1847.
- (31) Fiorentino, A.; D'Abrosca, B.; Pacifico, S.; Mastellone, C.; Scognamiglio, M.; Monaco, P. Identification and assessment of antioxidant capacity of phytochemicals from kiwi fruits. *J. Agric. Food Chem.* **2009**, *57*, 4148–4155.
- (32) Dawes, H. M.; Keene, J. B. Phenolic composition of kiwifruit juice. *J. Agric. Food Chem.* **1999**, *47*, 2398–2403.
- (33) Crowhurst, R. N.; Gleave, A. P.; MacRae, E. A.; Ampomah-Dwamena, C.; Atkinson, R. G.; Beuning, L. L.; Bulley, S. M.; Chagne, D.; Marsh, K. B.; Matich, A. J.; Montefiori, M.; Newcomb, R. D.; Schaffer, R. J.; Usadel, B.; Allan, A. C.; Bolding, H. L.; Bowen, J. H.; Davy, M. W.; Eckloff, R.; Ferguson, A. R.; Fraser, L. G.; Gera, E.; Hellens, R. P.; Janssen, B. J.; Klages, K.; Lo, K. R.; MacDiarmid, R. M.; Nain, B.; McNeilage, M. A.; Rassam, M.; Richardson, A. C.; Rikkerink, E. H. A.; Ross, G. S.; Schröder, R.; Snowden, K. C.; Souleyre, E. J. F.; Templeton, M. D.; Walton, E. F.; Wang, D.; Wang, M. Y.; Wang, Y. Y.; Wood, M.; Wu, R.; Yauk, Y. K.; Laing, W. A. Analysis of expressed sequence tags from *Actinidia*: applications of a cross species EST database for gene discovery in the areas of flavor, health, color and ripening. *BMC Genomics* **2008**, *9*, 1–26.
- (34) Walton, E. F.; De Jong, T. M. Growth and compositional changes in kiwifruit berries from three Californian locations. *Ann. Bot.* **1990**, *66*, 285–298.
- (35) Pero, R. W.; Lund, H. Dietary quinic acid supplied as the nutritional supplement AIO + AC-11® leads to induction of micromolar levels of nicotinamide and tryptophan in the urine. *Phytother. Res.* **2011**, *25*, 851–857.
- (36) Calvani, R.; Miccheli, A.; Capuani, G.; Tomassini, A.; Miccheli, A.; Puccetti, C. Gut microbiome-derived metabolites characterize a peculiar obese urinary metabotype. *Int. J. Obesity* **2010**, *34*, 1095–1098.
- (37) Villarino, M.; Sandín-Espana, P.; Melgarejo, P.; De Cal, A. High chlorogenic and neochlorogenic acid levels in immature peaches reduce monilinia laxa infection by interfering with fungal melanin biosynthesis. *J. Agric. Food Chem.* **2011**, *59*, 3205–3213.
- (38) Figueredo, A.; Fortes, A. M.; Ferreira, S.; Sebastiana, M.; Choi, Y. H.; Sousa, L.; Acioli-Santos, Pessoa, F.; Verpoorte, R.; Pais, M. S. Transcriptional and metabolic profiling of grape (*Vitis vinifera* L.) leaves unravel possible innate resistance against pathogenic fungi. *J. Exp. Bot.* **2008**, *59*, 3371–3381.
- (39) Hills, B. P.; Remigereau, B. NMR studies of changes in subcellular water compartmentation in parenchyma apple tissue during drying and freezing. *Int. J. Food Sci. Technol.* **1997**, *32*, 51–61.